Pergamon

*Int. J. Heat Mass Transfer.* Vol. 41, No. 13, pp. 1945–1954, 1998

Printed in Great Britain
0017-9310/98 $19.00+0.00

PII: S0017-9310(97)00301-3

# Constructal theory of natural crack pattern formation for fastest cooling

A. BEJAN,† Y. IKEGAMI‡ and G. A. LEDEZMA†

† Department of Mechanical Engineering and Materials Science, Box 90300, Duke University, Durham, NC 27708-0300, U.S.A. and ‡ OTEC Laboratory, Faculty of Science and Engineering, Saga University, 1 Honjo-machi, Saga-shi, Saga, 840, Japan

(*Received* 25 *July* 1997 *and in final form* 24 *September* 1997)

**Abstract**—The constructal theory of the origin of geometrical form in natural flow systems is used to predict the formation of crack patterns in solids subjected to volumetric cooling by convection. The approach is purely theoretical (deterministic), because it starts from the principle of geometric minimization of resistance to flow, and leads to the existence of optimal distances between successive cracks and, consequently, optimal crack widths. The analytical part of the paper is based on the method of intersecting the asymptotes (many cracks vs. few cracks), and anticipates several natural features that had not been explained previously: cracks are denser when the convective cooling effect is more intense and/or the initial departure from equilibrium is greater, and the loops are close to round (or square) in two-dimensional lattices of cracks. These trends are further illustrated by using a one-dimensional numerical conduction model with equidistant parallel-plate cooling channels. © 1998 Elsevier Science Ltd. All rights reserved.

## 1. OBJECTIVE

It was shown recently [1, 2] that by minimizing geometrically the thermal resistance between one point and a finite-size volume (an infinity of points) it is possible to predict a most common natural structure that previously was considered nondeterministic: the tree network. Tree network patterns abound in nature, in both animate and inanimate systems (e.g., botanical trees, river basins, lungs, vascularized tissues, lightning, neural dendrites, dendritic crystals). The key to solving this famous problem was the optimization of the shape of each finite-size element of the flow volume, such that the flow resistance of the element is minimal. The optimal structure of the flow was then constructed by putting together the shape-optimized building blocks. The structure was determined in time, by proceeding from small to large. Shapelessness (diffusion) came first, and geometrical form (channels) came later. This characteristic is worth repeating: disorganized flow (diffusion) came first and organized flow (channels) came later. This geometric optimization method was named 'constructal theory'.

The deterministic power of constructal theory is an invitation to new theoretical work on natural flow structures that have evaded determinism in the past. This paper is about one such flow: the natural formation of a pattern of cracks in a shrinking solid (Fig. 1). The constructal approach employed in this paper is based on the view that an occurring flow—its geometric structure—is the end result of a process of internal geometric optimization. The objective of the optimization process is to construct an assembly of paths of minimal resistance for the current (heat, fluid, mass) that is forced to flow through the system. We show that macroscopic shape and structure can be predicted based on the geometric minimization of flow resistance. In other words, we show that the constructal approach is deterministic with respect to the very existence of geometrical form.

The present extension of constructal theory is very timely because a large segment of the physics and biology communities works on identifying the physics principle that controls geometric form in natural systems, both animate and inanimate. This challenge was summarized by Kadanoff [3] in his critique of the proliferation of computer simulations (e.g., fractal algorithms) of naturally occurring structures. Kadanoff wrote that "further progress depends upon establishing a more substantial theoretical base in which geometrical form is deduced from the mechanisms that produce it". The constructal (geometric optimization) principle invoked in this paper answers this challenge, and shows that geometrical form can indeed by deduced from a single principle.

## 2. ANALYSIS

The formation of cracks in solids in an old and busy field that so far has been dug mainly by materials scientists, physicists and chemists. Many important advances have been made (e.g. refs. [4–6]), and these are backed by a voluminous literature. The challenge that persists is to explain the origin of such patterns, i.e., to predict their very existence. During the past decade it has become fashionable to describe cracking patterns in terms of fractal images. This tool is descriptive, not predictive.

## NOMENCLATURE

| | |
|---|---|
| $B$ | dimensionless group, equation (23) |
| $c$ | solid specific heat |
| $c_p$ | fluid specific heat at constant pressure |
| $D$ | crack size |
| $D_0$ | initial crack size |
| $k$ | solid thermal conductivity |
| $k_f$ | fluid thermal conductivity |
| $L$ | crack dimension in the direction of flow |
| $\dot{m}'$ | mass flow rate per unit length |
| $q'$ | heat transfer rate per unit length |
| $R$ | half distance between adjacent cracks |
| $S$ | dimensionless group, equation (23) |
| $t$ | time |
| $t_c$ | cooldown time |
| $T$ | temperature |
| $T_L$ | fluid inlet temperature |
| $T_H$ | solid initial temperature |
| $T_R$ | temperature of the cooled side |
| $U$ | mean velocity |
| $U_\infty$ | free stream velocity |
| $x$ | coordinate. |

Greek symbols

| | |
|---|---|
| $\alpha$ | solid thermal diffusivity |
| $\alpha_f$ | fluid thermal diffusivity |
| $\beta$ | coefficient of thermal contraction |
| $\delta$ | dimensionless crack size |
| $\delta_0$ | dimensionless initial crack size |
| $\Delta P$ | pressure difference |
| $\Delta T$ | temperature difference, $T_H - T_L$ |
| $\theta$ | dimensionless temperature |
| $\mu$ | viscosity |
| $\nu$ | kinematic viscosity |
| $\xi$ | dimensionless coordinate |
| $\rho$ | solid density |
| $\rho_f$ | fluid density |
| $\tau$ | dimensionless time |
| $\tau_c$ | dimensionless cooldown time. |

Subscripts

| | |
|---|---|
| min | minimal |
| opt | optimal |
| $R$ | the plane $x = R$ |
| 0 | the plane $x = 0$. |

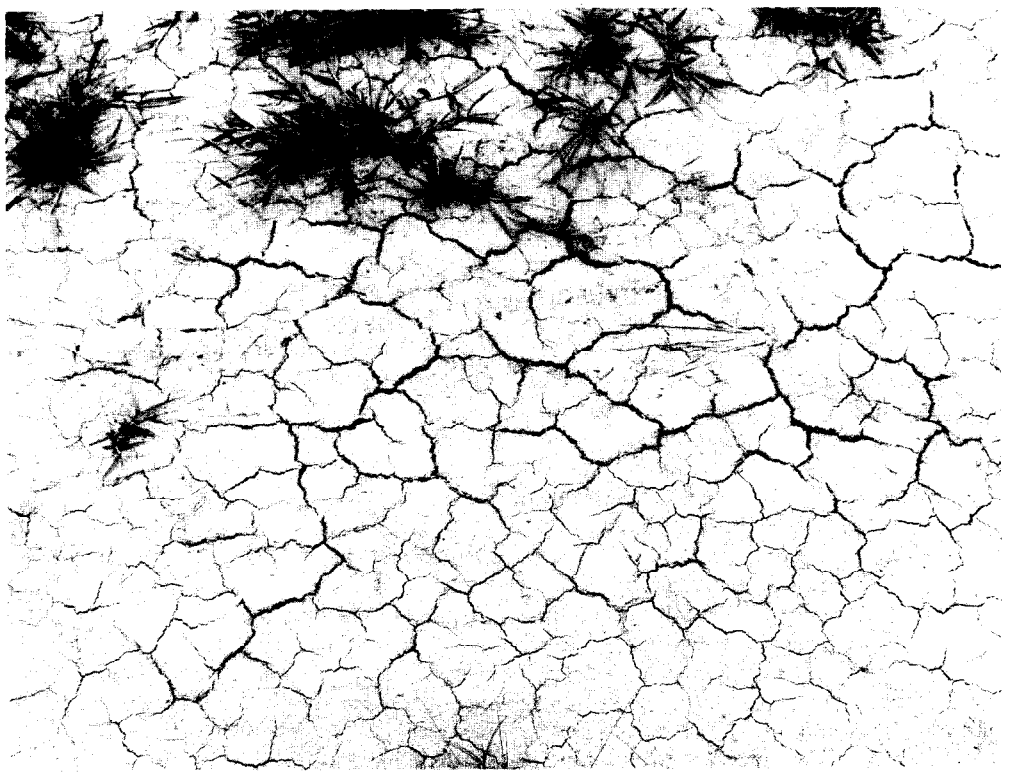

Fig. 1. Pattern of cracks on the ground.

Let us think freely about the most common example of patterned cracks, which is illustrated in Fig. 1. Wet soil exposed to the sun and the wind becomes drier, shrinks superficially, and develops a network of cracks. The loop in the network has a characteristic length scale. The loop is round, more like a hexagon or a square, not slender. The loop is smaller when the wind blows harder, that is when the drying rate is higher. A simple theory is needed for anticipating these extremely simple geometric characteristics.

These unexplained features of macroscopic cracks are major hints that their pattern is another natural occurrence of access optimization: the maximization of the mass transfer rate from the system (wet soil) to the ambient, or the minimization of the overall drying time. In view of the analogy between mass transfer and heat transfer, we can explore this theoretical route by considering the thermal analog of the system of Fig. 1. The simplest thermal analog is sketched in Fig. 2.

The existence of an optimal crack spacing for fastest cooling can be demonstrated based on 'the intersection of asymptotes method', which was developed in several geometric optimizations of the spacings of electronic packages (e.g., refs. [7–9]). Consider the one-dimensional conducting solid shown in Fig. 2. This is a very simple, highly idealized model: the closest connection between it and the example of Fig. 1 would be to imagine the view in a vertical cut through the soil, and to assume that the cracks continue downward to a depth $L$.

The cracks are spaced uniformly, however, the spacing scale $R$ is arbitrary at this point. In the plane perpendicular to the flow direction $\dot{m}'$, the cracks appear as parallel lines with a uniform spacing of size $2R$. The crack width $D$ increases in time, as each solid piece ($R$) shrinks. The cooling effect is provided by a single-phase fluid driven by the pressure difference $\Delta P$, which is maintained across the solid layer of thickness $L$.

The imposed pressure difference $\Delta P$ is an essential aspect of the crack spacing selection problem. For example, in the cooling of a hot dry rock deposit [10] a pressure difference is maintained between the water injected into the well and the pressure of the stream returned to ground level. In the air cooling of a vertical crack in the surface of a muddy terrain, the scale of $\Delta P$ is set at $(1/2)\rho_f U_\infty^2$, where $\rho_f$ and $U_\infty$ are the density and free-stream velocity of the external air flow (wind).

To examine the effect of the crack spacing $R$ on the time needed for cooling the solid, we consider the following two extremes.

### 2.1. *Many cracks*

When the number of cracks per unit length is large, the spacing $R$ is small and so is the eventual shrinkage that is experienced by each $R$ element. This means that in the limit $R \to 0$ we can expect $D \to 0$. In this limit, the flow through each $D$-thin crack is laminar (Hagen–Poiseuille), such that the crack mass flow rate is given by

$$\dot{m}' = \rho_f D U \sim \rho_f D \frac{D^2 \Delta P}{\mu L}. \tag{1}$$

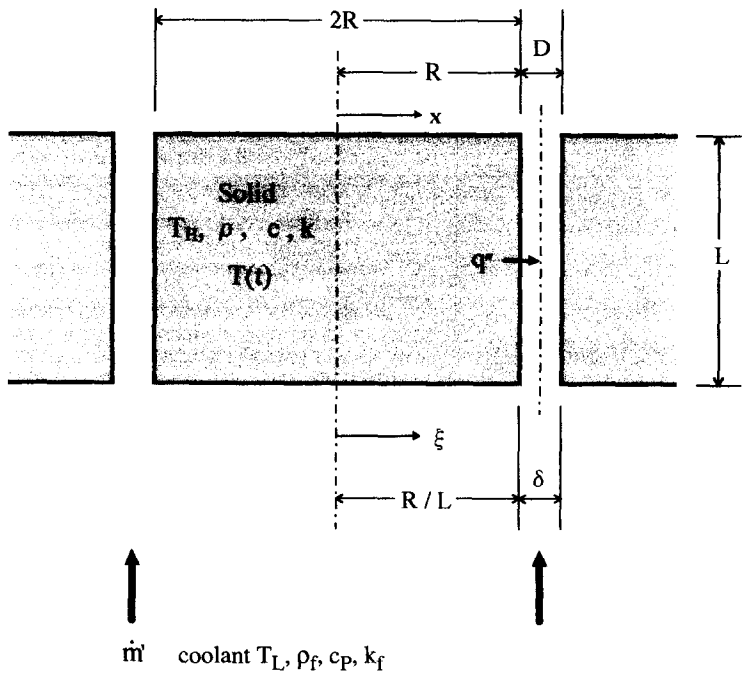


Fig. 2. Solid layer with equidistant cracks ($D$, $L$) cooled by single-phase convection.

In the same limit, $R$ is small enough so that the solid conduction is described by the lumped thermal capacitance model [11]. The solid piece $R$ is characterized by a single temperature $T$, which decreases in time from the initial level $T_H$ to the inlet temperature of the fluid, $T_L$. This cooling effect is governed by the energy balance

$$\rho c R L \frac{dT}{dt} = -q' \tag{2}$$

where $\rho$ and $c$ are the density and specific heat of the solid. The cooling effect ($q'$) provided by the flow through the crack is represented well by

$$q' = \dot{m}' c_p (T - T_L) \tag{3}$$

where $c_p$ is the specific heat of the coolant. By writing equation (3) we are recognizing that in the $D \to 0$ limit the fluid becomes as warm as the surrounding solid before it reaches the end of the crack. If we combine equations (2) and (3) we obtain the order of magnitude statement

$$\rho c R L \frac{\Delta T}{t} \sim \dot{m}' c_p \Delta T \tag{4}$$

where $\Delta T$ is the scale of the instantaneous solid excess temperature $T - T_L$. Finally, by using the $\dot{m}'$ scale provided by equation (1), we conclude that the cooling time scale is

$$t \sim \frac{\rho c}{\rho_f c_p} \frac{\mu R L^2}{D^3 \Delta P} \quad (R \to 0). \tag{5}$$

2.2. *Few cracks*

In the opposite limit, $R$ is large and the crack width $D$ is potentially very large—in proportion to $R$. The fluid present at one time in the crack is mainly isothermal at the inlet temperature $T_L$. The aspect that is more relevant to the present time-scale analysis is that when $R$ is sufficiently large the cooling of each solid side of the crack is ruled by one-dimensional thermal diffusion into a semiinfinite medium [11]. The cooling time is the same as the time of thermal diffusion (penetration) over the distance $R$,

$$t \sim \frac{R^2}{\alpha} \quad (R \to \infty) \tag{6}$$

where $\alpha = k/(\rho c)$, and $k$ is the thermal conductivity of the solid.

2.3. *The intersection of the asymptotes*

Figure 3 summarizes the scaling trends uncovered for $R \to 0$ and $R \to \infty$. According to equation (5), in the limit $R \to 0$ the cooling time is proportional to $R/D^3$ or $R^{-2}$, because $D$ and $R$ must be proportional,

$$\frac{D}{R} \sim \beta \Delta T \ll 1. \tag{7}$$

In this proportionality, $\Delta T \sim T_H - T_L$, and $\beta$ is the coefficient of linear thermal contraction of the solid. In the opposite limit ($R \to \infty$), the cooling time is proportional to $R^2$. Put together, these two proportionalities suggest that the cooling time possesses a sharp (important) minimum with respect to $R$ or the crack density. Intersecting equations (5) and (6) we find that the optimal crack distance ($R_{opt}$) for fastest cooling is of the order of

$$R_{opt} \sim \left[ \frac{k}{k_f} \frac{\alpha_f \nu L^2}{U_\infty^2 (\beta \Delta T)^3} \right]^{1/4}. \tag{8}$$

This result is promising for two fundamental reasons, in addition to the practical aspect of knowing how to extract heat from a solid in the fastest way possible. One reason is that the optimal crack distance decreases as the external pressure (or flow) is intensified. This effect is in accord with observations that mud cracks become denser when the wind speed increases [4]. Equation (8), in association with the constructal principle that natural cracks occur such that the cooling speed is maximized, is the first theoretical prediction of the effect of wind speed on crack density.

The second reason why equation (8) is important fundamentally is that it predicts a higher density of cracks (a smaller $R_{opt}$) as the solid excess temperature $\Delta T$ increases. This trend too is in agreement with the large volume of observations recorded in the materials science literature [4–6]. Again, equation (8) and the time minimization theory presented in this section predict the dependence of the cooldown time on the initial temperature difference.

## 3. NUMERICAL FORMULATION

The theoretical trends discovered in the preceding section can be described in more concrete terms by simulating numerically the heat transfer and solid contraction processes. The numerical formulation is based on the unidirectional conduction and coordinate system model shown in Fig. 2. The crack opening increases in time, $D(t)$, however, it is much smaller than the solid dimension $R$, such that $R$ can be regarded as being practically time-independent. Because of symmetry, it is sufficient to calculate the temperature distribution $T(x, t)$ in the solid piece situated between $x = 0$ and $x = R$. The energy equation

$$\frac{1}{\alpha} \frac{\partial T}{\partial t} = \frac{\partial^2 T}{\partial x^2} \tag{9}$$

is subjected to the initial and boundary conditions

$$T = T_H \quad \text{at } t = 0 \tag{10}$$

$$\frac{\partial T}{\partial x} = 0 \quad \text{at } x = 0 \tag{11}$$

$$2q''L = \dot{m}' c_p (T_R - T_L) \quad \text{at } x = R \tag{12}$$

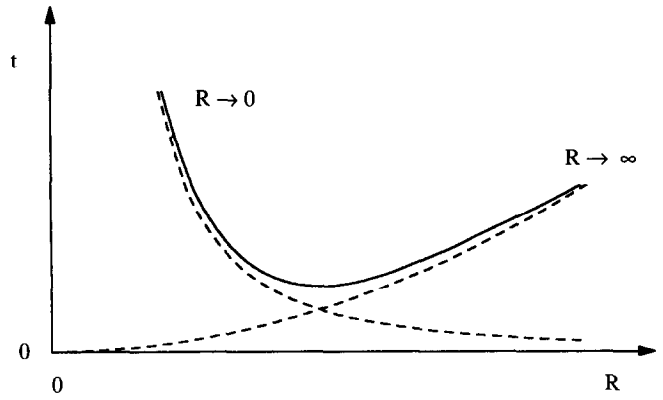


Fig. 3. The minimal cooldown time at the intersection of the $R \to 0$ and $R \to \infty$ asymptotes.

where $q'' = -k(\partial T/\partial x)_R$. The exact form of equation (1) for Hagen–Poiseuille flow,

$$\dot{m}' = \rho_f D \frac{D^2}{12\mu} \frac{\Delta P}{L} \tag{13}$$

allows us to rewrite equation (12) as

$$-k\left(\frac{\partial T}{\partial x}\right)_R L = \frac{D^3}{24\nu} \frac{\Delta P}{L} c_p (T_R - T_L). \tag{14}$$

The growth of $D(t)$, or the shrinking of the solid, is described by

$$D(t) = D_0 + 2\int_0^R \beta[T_H - T(x,t)]\,dx \tag{15}$$

where $D_0$ is the initial (very small) size of $D$.

The nondimensionalization of the conduction problem statement is based on using $L$ and $T_H - T_L$ as length and temperature change scales:

$$\xi = \frac{x}{L} \quad \theta = \frac{T - T_L}{T_H - T_L} \tag{16}$$

$$\tau = \frac{t\alpha}{L^2} \quad \delta = \frac{D}{L}. \tag{17}$$

Equations (9)–(11) and (14) become

$$\frac{\partial \theta}{\partial \tau} = \frac{\partial^2 \theta}{\partial \xi^2} \tag{18}$$

$$\theta = 1 \quad \text{at } \tau = 0 \tag{19}$$

$$\frac{\partial \theta}{\partial \xi} = 0 \quad \text{at } \xi = 0 \tag{20}$$

$$-\frac{\partial \theta}{\partial \xi} = B\delta^3 \theta_R \quad \text{at } \xi = R/L \tag{21}$$

$$\delta = \delta_0 + 2S\int_0^{R/L} (1-\theta)\,d\xi \tag{22}$$

where $\theta_R = (T_R - T_L)/(T_H - T_L)$. The dimensionless groups $B$ and $S$ account for the forced flow and shrinking characteristics of the solid,

$$B = \frac{L^2 c_p \Delta P}{24\nu k} \quad S = \beta(T_H - T_L). \tag{23}$$

Equation (18) was solved using a Crank–Nicolson Scheme, which is second order accurate in both time and space [12]. Equation (22) was integrated in each time step using a trapezoidal rule. We used 201 equidistant nodes to discretize $\xi$ when $0 < \xi \leqslant 2$. The error was checked against a fourth order solution (in space) obtained by using Richardson extrapolation based on a solution with 201 nodes and another solution with 401 nodes.

The shrinking of the solid was simulated by solving equation (22) at each time step. After updating the size of the domain the nodal points (always equidistant) were relocated. It was assumed that the contraction is very small such that the temperature in each nodal point is approximated well by the temperature at the same node before each update of the domain size. Figure 4 shows that the contraction is in fact very small relative to $R/L$.

An initial thickness of the crack ($\delta_0$) had to be assumed in order to make the heat flux at $\xi = R/L$ finite. We found that $\delta_0$ must be in the range $10^{-7} \leqslant \delta_0 \leqslant 10^{-5}$. The Fourier number based on the node spacing was $10^2 \leqslant \Delta\tau/(\Delta\xi)^2 \leqslant 10^6$. The boundary condition (21) was implemented by requiring $-\partial\theta/\partial\xi = B\delta^3\theta_R$ when $\theta_R > 0$, and $\theta = 0$ when $\theta_R = 0$.

## 4. NUMERICAL RESULTS

The behavior of the temperature distribution in the solid $\theta(\tau, \xi)$ is illustrated in Fig. 5. The distribution is initially isothermal. The side that is in contact with the coolant ($\xi = 1$) drops relatively fast to the inlet temperature of the fluid ($\theta = 0$). The temperature in the center of the solid piece ($\theta_0$ at $\xi = 0$) is the last to decrease. We used the time decay of $\theta_0$ to monitor the progress made by the cooldown process. By convention, the cooldown time $\tau_c$ was defined when $\theta_0$ dropped to 10% of its initial value:

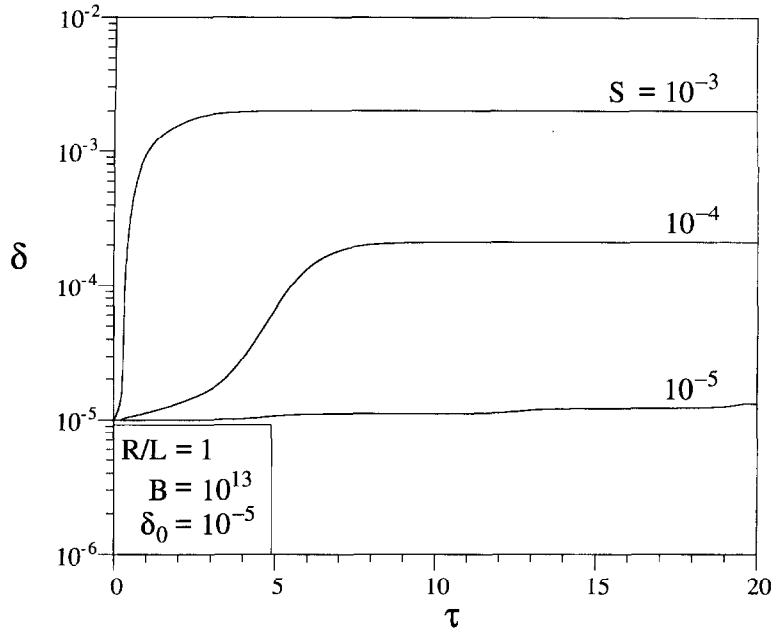


Fig. 4. Time evolution of the relative contraction of the solid system of Fig. 2.

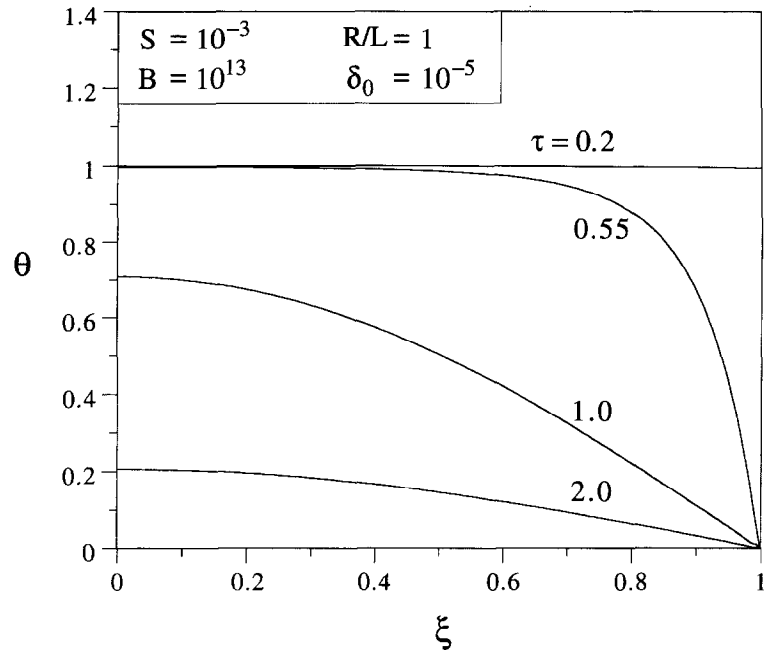


Fig. 5. The history of the temperature distribution in the solid during the cooldown process.

$$\theta_0(\tau_c) = 0.1. \tag{24}$$

Figure 6 shows another view of the history of the cooldown process. The channel opening $\delta$ increases relatively abruptly, and this causes a jump in the coolant flow rate and the associated heat removal rate. The dimensionless heat flux shown with dashed line is $q_R = -(\partial\theta/\partial\xi)_\xi = R/L$. After the jump in $\delta$, the cooling rate $q_R$, center temperature $\theta_0$ and side temperature $\theta_R$ decrease monotonically. The channel size $\delta$ approaches the plateau associated with the uniform cooling (shrinking) of the solid to $\theta = 0$ at $\tau \to \infty$.

The cooldown process depends on the three dimensionless groups: $R/L$, $B$ and $S$. Of primary interest is the effect of the geometric parameter $R/L$, which accounts for the spacing between adjacent cracks. Fig-

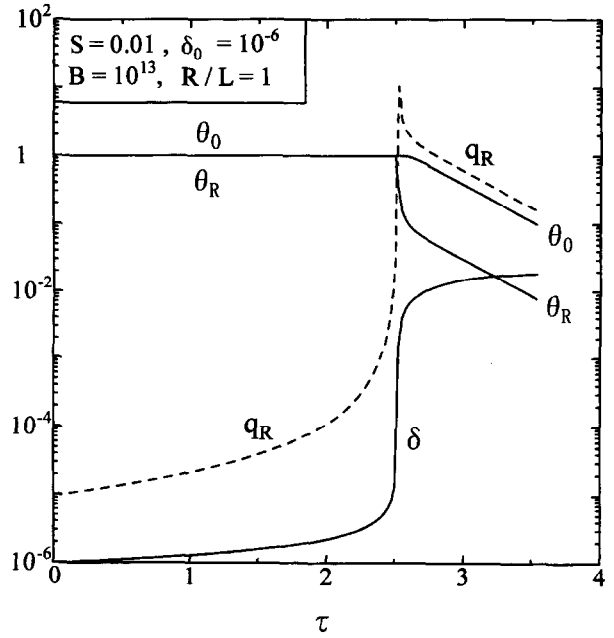


Fig. 6. The evolution of the channel opening $\delta$, cooling rate $q_R$, center temperature $\theta_0$, and channel side temperature $\theta_R$.

ure 7 shows the effect of $R/L$ on the calculated cooldown time $\tau_c$. The minimum exhibited by $\tau_c$ confirms the behavior anticipated in Fig. 3, however, in the numerical results the $\tau_c$ minimum is shallow and less pronounced on the side that corresponds to small $R/L$ values. The minimal cooldown time is indicated by a circle on each of the $\tau_c$ curves of Fig. 7(a)–(c). The value $\tau_{c,min}$ increases as the imposed pressure difference ($B$) decreases [Fig. 7(a)] and as the shrinkage parameter $S$ decreases [Fig. 7(b)].

To solve the time-dependent conduction problem numerically it was necessary to assume the existence

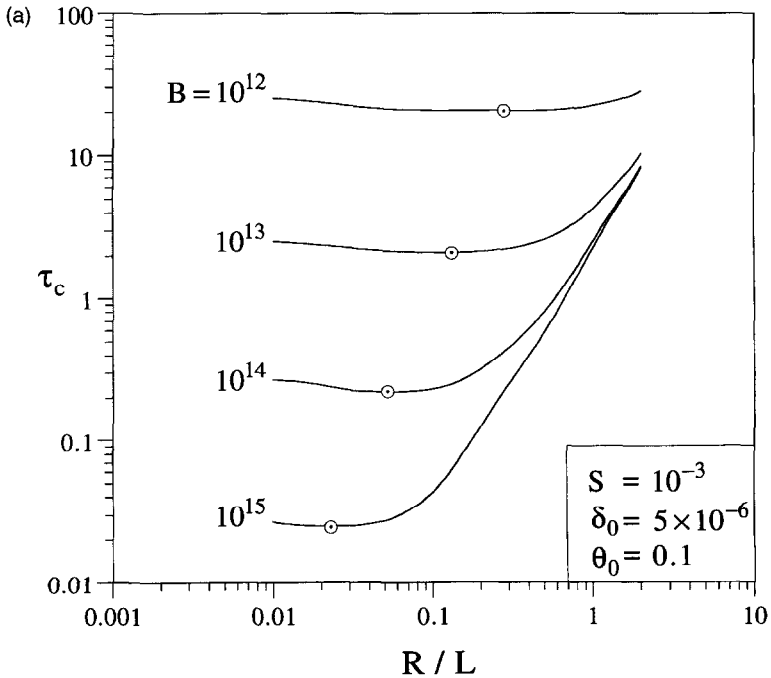


Fig. 7. The effect of the crack-to-crack spacing $R/L$ on the cooldown time, and the influence of $B$, $S$ and $\delta_0$.

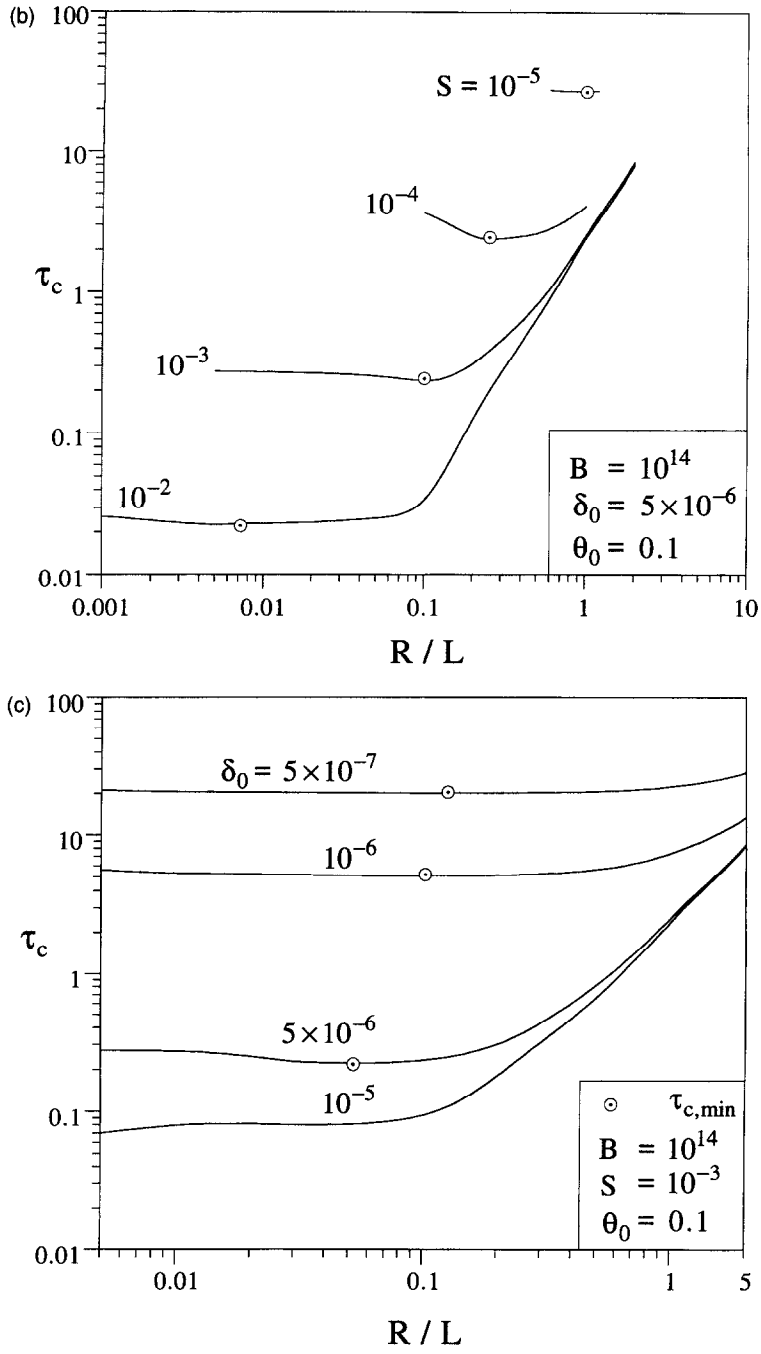


Fig. 7—*continued.*

of a small but finite crack opening ($\delta_0$) when the numerical simulation begins ($\tau = 0$). In Figs. 6 and 7 this starting value was $\delta_0 \sim O(10^{-6})$, which is about four orders of magnitude smaller than the value approached by the crack size $\delta$ as $\tau$ becomes large. The choice of $\delta_0$ influences the calculated value of $\tau_{c,min}$. Figure 7(c) shows that the minimal cooldown time decreases as $\delta_0$ increases, and that when $\delta_0$ is greater than $O(10^{-5})$ the $\tau_c$ minimum disappears.

The trends exhibited by $\tau_c$ in Fig. 7(a)–(c) can be summarized by correlating the minimal cooldown time $\tau_{c,min}$ and optimal spacing $R_{opt}/L$ as functions of $B$, $S$ and $\delta_0$. For example, the results of Fig. 7(a) can be used to conclude that $\tau_{c,min}$ is approximately proportional to $B^{-1}$ and $R_{opt}/L$ is proportional to $B^{-1/3}$. The results of Fig. 7(b) show that $\tau_{c,min} \approx S^{-1}$ and $R_{opt}/L \sim S^{-2/3}$. Finally, Fig. 7(c) shows that $\tau_{c,min}$ and $R_{opt}/L$ vary as $\delta_0^{-2}$ and, respectively, $\delta_0^{-3/10}$. In sum, the numerical results presented in this section are correlated within 13% by the expression

$$\frac{R_{opt}}{L} = 1.93B^{-0.4}S^{-0.73}\delta_0^{-0.34} \tag{25}$$

and within 6% by

$$\tau_{c,min} = 0.45B^{-0.97}S^{-1.02}\delta_0^{-1.93}. \tag{26}$$

These trends agree qualitatively with the predictions made by intersecting the $R \to 0$ and $R \to \infty$ asymptotes in Section 2. Transformed in the dimensionless notation of equations (23), the $R_{opt}$ estimate of equation (8) reads

$$\frac{R_{opt}}{L} \sim B^{-1}S^{-3}. \tag{27}$$

The numerical correlation (25) points in the same direction, however, the dependence of $R_{opt}/L$ on $B$ and $S$ is weaker.

Another prediction based on the analysis of Section 2 [equation (8)] is that the minimal cooldown time is $t_{c,min} \sim R_{opt}^2/\alpha$, cf. equations (6) or (5). This prediction is also written as $\tau_{c,min} \sim (R_{opt}/L)^2$, and is supported qualitatively by the numerical correlations (25) and (26). Note that by squaring the right side of equation (25) we obtain an expression that approaches equation (26). Not anticipated by the analysis of Section 2 is the effect of the crack start-up value $\delta_0$. This effect requires further study, to decide whether it is a feature of the cooldown phenomenon or the fingerprint of the simplicity of the numerical one-dimensional heat conduction model (Fig. 2).

## 5. TWO-DIMENSIONAL CRACK PATTERNS

The constructal principle of geometric optimization of access to equilibrium was demonstrated in Sections 2–4 by using the simplest conduction heat transfer model: unidirectional time-dependent conduction. The same principle can be investigated by using a two-dimensional time-dependent conduction model. For example, as shown in the two-dimensional example of Fig. 1, the cracks would form a pattern (a lattice) in the plane perpendicular to the flow direction. The challenge is to determine not only the optimal length scale of the pattern (i.e., the size of the loop in the lattice) but also the optimal shape of the loop (i.e., should the loop be elongated, or closer to a square?).

Theoretical progress on the two-dimensional pattern can be made based on the conclusions of Section 2. Specifically, an important geometric implication of equation (8) is that the optimal distance between consecutive cracks must increase as $L^{1/2}$. This result is relevant to predicting the length scale of the lattice of vertical cracks formed in a horizontal two-dimensional surface cooled (or dried) under the influence of external forced convection (e.g. wind). Since the direction of the air flow may change locally from time to time, and since the material (its graininess) may be such that cracks may propagate in all directions, we arrive at the problem of cooling a two-dimensional terrain (area $A$, when seen from above) with cracks of length $L$ and associated spacings $R_{opt}$.

Figure 8 shows the two extremes in which $L$ may find itself in relation to $R_{opt}$. First, when $L$ is considerably shorter than $R_{opt}$ [Fig. 8(a)] it is impossible to cover the area $A$ exclusively with patches of size $L \times R_{opt}$. The reason is that when two cracks of length $L$ are joined (at an angle), the elemental area trapped between them (the area of order $L^2$) is too small to accommodate the amount of ideally cooled solid material.

When $L$ is considerably longer than $R_{opt}$ [Fig. 8(b)], any lattice of cracks will fail to cover the area $A$ completely. The reason is that the trapped elemental area ($\sim L^2$) is considerably larger than the amount of ideally cooled solid ($\sim LR_{opt}$). Geometrically, this means that most of the interior of the element $L^2$ would require a cooling time that is considerably longer than the minimum time determined in equation (8).

In conclusion, to cool the entire solid ($A$) in the fastest way possible is to cover the $A$ cross-section with $L \times R_{opt}$ elements in which $L \sim R_{opt}$, i.e., elements with 'round' shape. Combining $L \sim R_{opt}$ with equation (8) we find the optimal length scale of the element (loop) in the network of cracks that will minimize the cooldown time,

$$R_{opt}^2 \sim \frac{(\alpha_f \nu k/k_f)^{1/2}}{U_\infty(\beta\Delta T)^{3/2}}. \tag{28}$$

We see once again that, in agreement with observations [4], the lattice length scale $R_{opt}$ decreases as the wind speed and the initial excess temperature increase.

## 6. CONCLUSION

The theoretical and numerical work reported in this paper provides a deterministic basis for the existence of an optimal spacing between cracks in solids that simultaneously undergo cooling and volumetric shrinking. An optimal crack-to-crack spacing corresponds to the minimal cooldown time. In other words, the regularly spaced cracks are the geometric pattern that allows the solid to reach its new equilibrium state ($T = T_L$, uniform) in the fastest way possible.

This deterministic development is important for several reasons. With respect to the natural formation of crack patterns in solids, which is a large and mature field of study, the work presented in this paper anticipates for the first time that (a) cracks are denser when the convective cooling effect is more intense [e.g., $U_\infty$ in equation (8)], (b) cracks are denser when the initial departure from equilibrium is larger [e.g., $\Delta T$ in equation (8)], and (c) the loops are close to round (or square) in two-dimensional lattices of cracks.

These conclusions extend constructal theory to a new class of naturally organized systems: natural, macroscopic crack patterns in solids. There is an

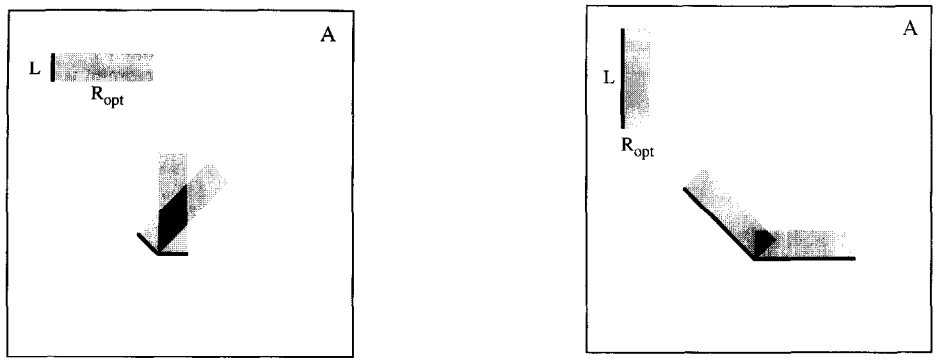


(a) (b)

Fig. 8. The fastest cooling of a two-dimensional solid that contracts volumetrically, or how to cover completely an area ($A$) with a lattice of cracks ($L$) and solid material of optimal thickness ($R_{opt}$).

important technological aspect to this new work, which becomes visible if we compare the optimized crack distribution of a cooling solid such as Fig. 2 with the optimized internal architecture of an electronic package. The optimized unit $R \times L$ of Fig. 2 is an 'elemental system' in the sense of constructal theory [1]: volumetric diffusion is balanced optimally by channelled flow (streams), in such a way that the diffusion mechanism touches every point of the volume. In other words, two heat-flow regimes are needed (diffusion and streams), and the one with the highest resistance (diffusion) is assigned to the scales that are smaller than the smallest channel. Artificial systems (e.g., electronic packages) owe their internal geometric form to the same physics principle as natural systems (e.g., cracked solids): the geometric minimization of resistance to flow subject to overall constraints (size, current). Additional applications of constructal theory are reviewed in a new book [13].

*Acknowledgements*—This work was sponsored by the National Science Foundation (U.S.A.) and the Ministry of Education (Japan).

## REFERENCES

1. Bejan, A., Constructal-theory network of conducting paths for cooling a heat generating volume. *International Journal of Heat and Mass Transfer*, 1997, **40**, 799–816.
2. Ledezma, G. A., Bejan, A. and Errera, M. R., Constructal tree networks for heat transfer. *Journal of Applied Physics*, 1997, **82**(1), 89–100.
3. Kadanoff, L. P., Fractals: where's the physics? *Physics Today*, 6–7 February 1986.
4. Walker, J., Cracks in a surface look intricately random but actually develop rather systematically. *Scientific American*, 1986, **255**, 204–209.
5. Meakin, P., Models for material failure and deformation. *Science*, 1991, **252**, 226–234.
6. Yakobson, B. I., Morphology and rate of fracture in chemical decomposition of solids. *Physical Review Letters*, 1991, 1590–1593.
7. Bejan, A. and Sciubba, E., The optimal spacing of parallel plates cooled by forced convection. *International Journal of Heat and Mass Transfer*, 1992, **35**, 3259–3264.
8. Anand, N. K., Kim, S. H. and Fletcher, L. S., The effect of plate spacing on free convection between heated parallel plates. *Journal of Heat Transfer*, 1992, **114**, 515–518.
9. Petrescu, S., Comments on the optimal spacing of parallel plates cooled by forced convection. *International Journal of Heat and Mass Transfer*, 1994, **37**, 1283.
10. Lim, J. S., Bejan, A. and Kim, J. H., Thermodynamic optimization of phase-change energy storage using two or more materials. *Journal of Energy Research Technology*, 1992, **114**, 84–90.
11. Bejan, A., *Heat Transfer*. Wiley, New York, 1993.
12. Fletcher, C. A. J., *Computational Techniques for Fluid Dynamics*, Vol. 1. Springer-Verlag, Berlin, 1991.
13. Bejan, A., *Advanced Engineering Thermodynamics*, 2nd edn. Wiley, New York, 1997.